

Hydraulics of Flared End Sections for Pipe Culverts

BRUCE M. McENROE AND LANCE M. JOHNSON

The most common end sections for pipe culverts are the shop-fabricated metal end sections and precast concrete end sections available from pipe suppliers. However, the standard reference works on culvert hydraulics provide little information on their hydraulic performance. The hydraulic characteristics of common flared end sections were recently investigated in model tests conducted at the University of Kansas for the Kansas Department of Transportation. Inlet-control rating curves were developed and entrance-loss coefficients for metal and concrete flared end sections of all sizes were determined. The hydraulic effects of floating debris were investigated and some potential design improvements tested. Under inlet control, standard flared end sections perform much better than mitered pipes, slightly better than headwalls with sharp inlet edges, and slightly worse than headwalls with grooved or rounded inlet edges. The concrete flared end sections are slightly more efficient than the metal end sections. Entrance-loss coefficients for flared end sections range from 0.24 to 0.30. Floating debris has little effect on the hydraulic performance of the flared end sections under inlet control. However, an accumulation of debris alters the flow pattern in a way that can cause a shift from inlet control to full flow, a more efficient operating condition. The hydraulic performance of a flared inlet can be improved by adding several bars across the top third of the inlet opening. These "flow bars" have the same beneficial hydraulic effects as an accumulation of debris at the inlet.

The most common end sections for pipe culverts are the shop-fabricated metal end sections and precast concrete end sections available from pipe suppliers. However, the standard reference works on culvert hydraulics provide little information on the hydraulic characteristics of these common open flared end sections. The FHWA's report (1) contains only the following note: "End sections conforming to fill slope' made of either metal or concrete, are the sections commonly available from manufacturers. From limited hydraulic tests they are hydraulically equivalent in operation to a headwall in both inlet and outlet control."

The results of hydraulic model tests of culverts with metal and concrete flared end sections are presented in this paper. These tests were performed at the University of Kansas hydraulics laboratory for the Kansas Department of Transportation (KDOT). The objectives of these tests were to (a) develop inlet-control rating curves for the metal and concrete flared end sections used by KDOT, (b) determine the entrance-loss coefficients for full flow through these end sections, (c) determine how their hydraulic characteristics are affected by debris, and (d) explore design modifications that might improve their hydraulic performance.

B. M. McEnroe, Department of Civil Engineering, 2006 Learned Hall, University of Kansas, Lawrence, Kans. 66045. L. M. Johnson, White, Martin and Associates, Inc., Engineering Consultants, 1725 S. W. Gage Boulevard, Topeka, Kans. 66604.

EXPERIMENTAL PROCEDURES

Hydraulic tests were run on models of metal and concrete flared end sections for pipe culverts 61 cm (24 in.) and 152 cm (60 in.). Figure 1 and Table 1 show the geometry and prototype dimensions of the metal end sections. Figure 2 and Table 2 show the geometry and prototype dimensions of the concrete end sections. The designs of the metal and concrete end sections differ slightly. The concrete end sections have more gradual side flares and thicker inlet edges than the metal end sections. Two sizes were tested because flared end sections of different sizes have slightly different proportions: the larger the diameter, the smaller the length-to-diameter ratio. The four models were all scaled to fit a 15-cm (6-in.) pipe.

The models were tested in a glass-walled water flume that is 0.76 m (2.5 ft) wide, 0.91 m (3.0 ft) deep, and 18 m (60 ft) long. The model culvert was a 0.9-m (3-ft) section of 152-mm (6-in.) transparent acrylic pipe. The model culvert was installed through a circular opening in a headwall of aluminum plate. The longitudinal slope of the installed culvert was 0.02 ft/ft. An embankment of river gravel surrounded the upstream end section. The discharge was measured with a V-notch weir installed in the flume about 3 m (10 ft) upstream from the culvert. The bottom of the V-notch was 0.61 m (2.0 ft) above the bottom of the flume. A honeycomb baffle between the weir and the model culvert distributed the flow uniformly over the cross section of the flume. The head on the weir and the depths of flow upstream and downstream of the models were measured with point gauges.

PERFORMANCE UNDER INLET CONTROL

If a pipe culvert is operating under inlet control, the discharge (Q) is determined by the headwater depth (HW), and the geometry of the end section. The geometry of the end section is characterized by the diameter of the conduit (D), and several other dimensions represented by the variables x_1 through x_n . In mathematical form, the relationship is

$$Q = f(HW, \rho, \gamma, D, X_1, X_2, \dots, X_n) \quad (1)$$

in which ρ and γ are the density and specific weight of the water and $f(\)$ is a function that must be determined experimentally. Wall roughness, viscosity, and surface tension are neglected because these factors have little effect on the flow pattern through sharp-edged inlets, even at the model scale (2-6). Dimensional analysis leads to the dimensionless relationship

$$\frac{Q}{\sqrt{gD^5}} = f\left(\frac{HW}{D}, X_1, X_2, \dots, X_n\right) \quad (2)$$

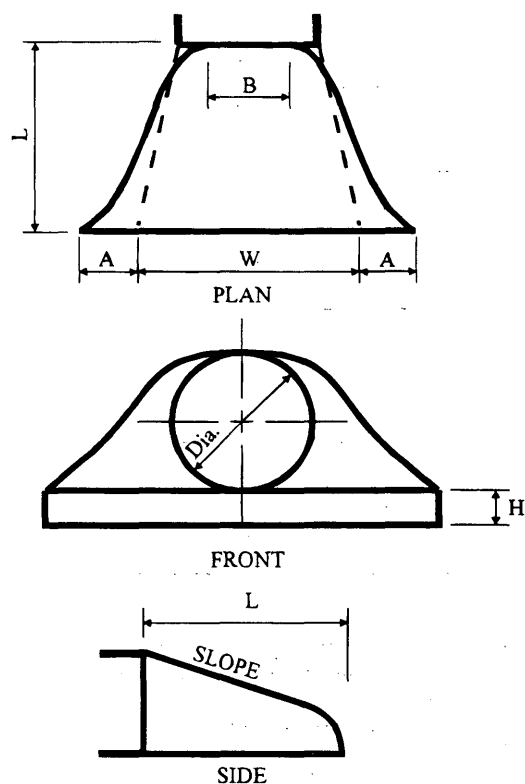


FIGURE 1 Geometry and dimensions of metal flared end sections.

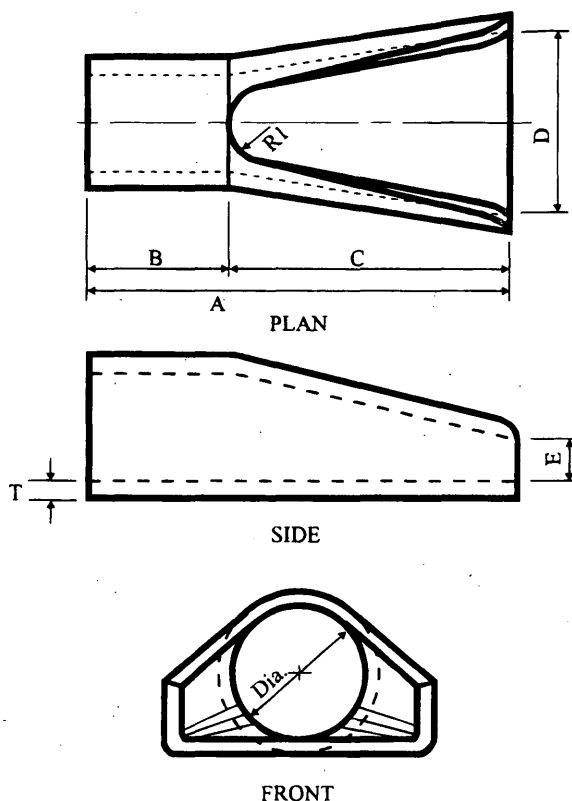


FIGURE 2 Geometry and dimensions of concrete flared end sections.

in which X_1 through X_n are dimensionless variables that describe the geometry of the end section. The dimensionless discharge, $Q/(gD^5)^{1/2}$, is a form of the Froude number. For geometrically similar end sections, the functional relationship is

$$\frac{Q}{\sqrt{gD^5}} = f\left(\frac{HW}{D}\right) \quad (3)$$

According to Equation 3, geometrically similar culverts with equal values of HW/D also have equal values of $Q/(gD^5)^{1/2}$. This relationship is used to convert the experimental results from the model scale to the prototype scale.

Each model was tested first under inlet control with no tailwater. The discharge in the flume was increased in steps. At each discharge, the head on the weir and the headwater level at the culvert were measured and recorded and the flow conditions at each end of the culvert were noted. The measured discharges and headwater depths were expressed in terms of the dimensionless variables

$$Q^* = \frac{Q}{\sqrt{gD^5}} \quad (4)$$

and

$$HW^* = \frac{HW}{D} \quad (5)$$

Each test was terminated at $HW/D = 4$, the point at which the headwater began to submerge the V-notch weir upstream.

When an end section became submerged by rising headwater, a vortex often formed where the end section connects to the pipe. Vortices were common for all end sections tested. None of the end sections caused the short smooth pipe to flow full.

Figure 3 compares the dimensionless rating curves for the 61-cm (24-in.) and 152-cm (60-in.) metal flared end sections. Figure 4 compares the dimensionless rating curves for the 61-cm (24-in.) and 152-cm (60-in.) concrete flared end sections. These comparisons show that the differences in the shapes of the 61-cm (24-in.) and 152-cm (60-in.) end sections have no significant effect on their hydraulic performance under inlet control. The curves defined by the data show a change in curvature near $HW/D = 1$, the level at which the inlet starts to become submerged. The dimensionless experimental data for the metal flared end sections are fitted closely by the equation

TABLE 1 Dimensions of Metal Flared End Section in Figure 1

Dia. (cm)	A (cm)	B (cm)	H (cm)	L (cm)	W (cm)	SLOPE
61	25	33	15	104	122	2.5:1
152	46	84	30	221	290	2:1

TABLE 2 Dimensions of Concrete Flared End Sections in Figure 2

Dia. (cm)	A (cm)	B (cm)	C (cm)	D (cm)	E (cm)	R1 (cm)	T
61	187	76	110	122	24	36	8
152	251	99	152	244	89	61	15

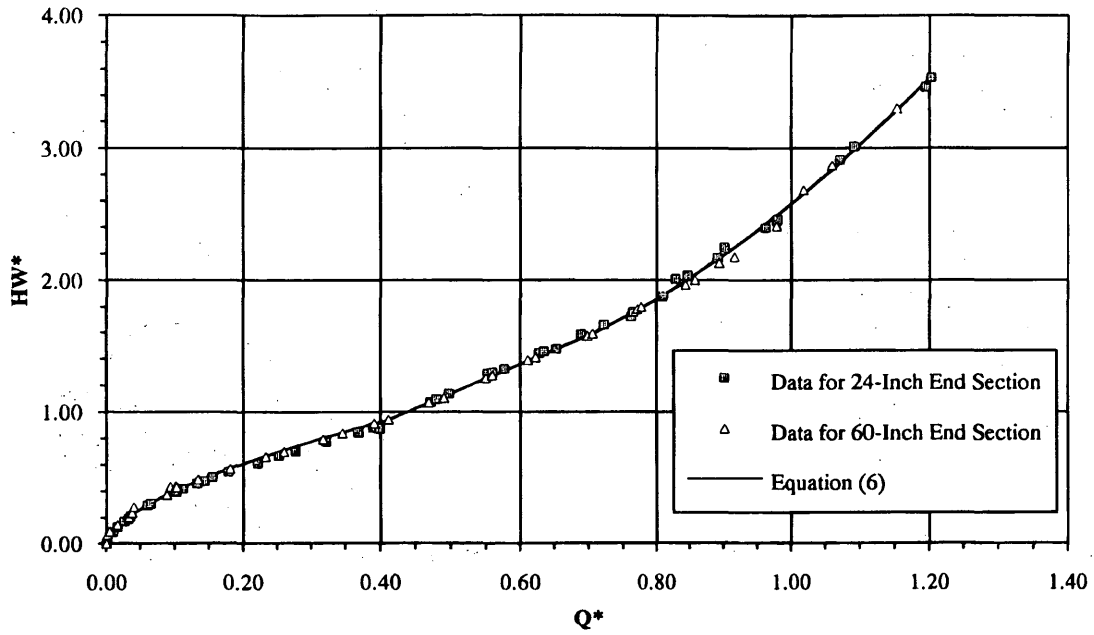


FIGURE 3 Hydraulic performance of metal flared end sections under inlet control.

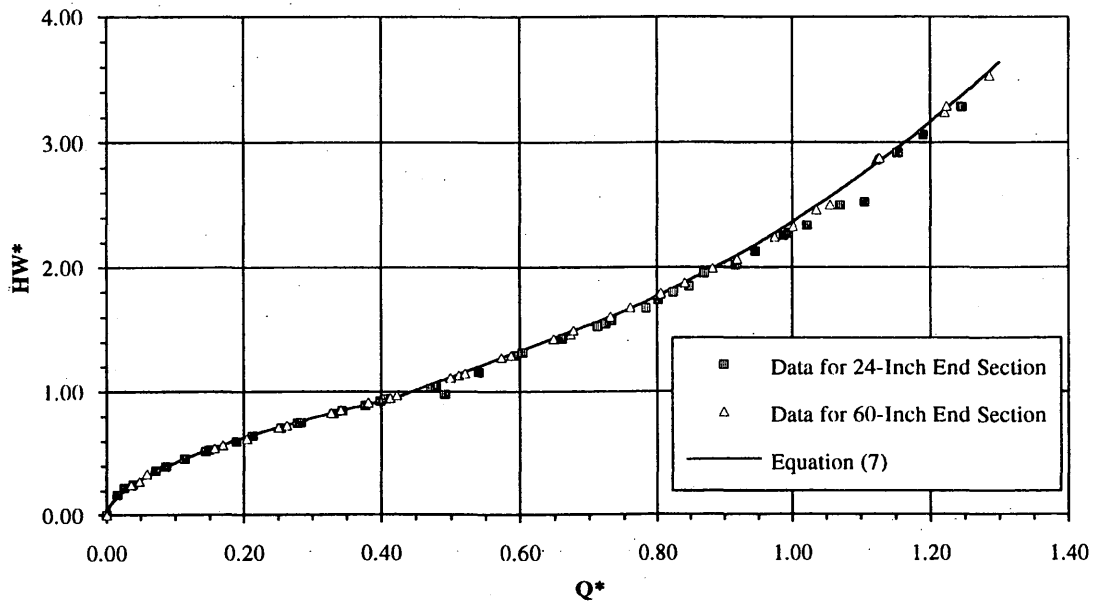


FIGURE 4 Hydraulic performance of concrete flared end sections under inlet control.

$$HW^* = \begin{cases} 1.60 (Q^*)^{0.60} & 0 \leq Q^* \leq 0.41 \\ 2.23 (Q^*) + 0.023 & 0.41 < Q^* \leq 0.62 \\ 1.289 - 1.61 (Q^*) + 2.90 (Q^*)^2 & 0.62 < Q^* \leq 1.20 \end{cases} \quad (6)$$

The dimensionless experimental data for the concrete flared end sections are fitted closely by the equation

$$HW^* = \begin{cases} 1.53 (Q^*)^{0.55} & 0 \leq Q^* \leq 0.42 \\ 2.13 (Q^*) + 0.055 & 0.42 < Q^* \leq 0.68 \\ 1.367 - 1.50 (Q^*) + 2.50 (Q^*)^2 & 0.68 < Q^* \leq 1.30 \end{cases} \quad (7)$$

Figure 5 provides a comparison of the dimensionless inlet-control rating curves for the metal and concrete flared end sections and the dimensionless forms of FHWA's rating curves for concrete pipes with headwalls and mitered corrugated metal pipes (*I*). The concrete end sections are slightly more efficient than the metal end sections when submerged. The two rating curves for the concrete pipes with headwalls (one with a sharp inlet edge, the other with a grooved edge) envelop the rating curves for the flared end sections. Both types of flared end sections are considerably more efficient than a mitered corrugated metal pipe.

ENTRANCE-LOSS COEFFICIENTS FOR FULL FLOW

To determine the entrance-loss coefficient for full flow, each model was tested with its outlet submerged by high tailwater. The headwater level, tailwater level, and head on the weir were measured at several different discharges. The entrance-loss coefficients were determined from an energy balance between the headwater pool and the outlet of the conduit. The friction loss through the pipe was computed with the Darcy-Weisbach formula. The Darcy-Weisbach friction factor was determined from the smooth pipe curve on the Moody diagram. Table 3 shows the experimentally determined values of the entrance-loss coefficients for full flow through each of the flared end sections.

TABLE 3 Entrance-Loss Coefficients for Flared End Sections

Diameter (cm)	Entrance-Loss Coefficient, K_e	
	Metal	Concrete
61	0.31	0.31
152	0.24	0.24

The 61-cm (24-in.) end sections have larger entrance-loss coefficients than the 152-cm (60-in.) end sections because the smaller sizes are longer (relative to the pipe diameter) and less flared. Metal and concrete flared end sections of the same size have identical entrance-loss coefficients. The experimentally determined entrance-loss coefficients are considerably lower than the value of 0.5 recommended for "end sections conforming to fill slope" in the FHWA report (*I*).

EFFECTS OF DEBRIS

The hydraulic tests of the model end sections were repeated with floating debris. In the initial test of each model with debris, loose twigs and straw were scattered on the bottom of the dry flume upstream of the end section. Then the discharge in the flume was increased slowly with no tailwater downstream of the culvert. More twigs and straw were scattered upstream of the end section as the discharge was increased. The headwater was allowed to rise until the debris floating on the water surface pulled free of any debris retained on the end section. Then the discharge in the flume decreased gradually to zero. At various stages as the headwater rose and then fell, the extent of any accumulation of debris in the end section was recorded.

These tests clearly showed the progression of events that leads to partial blockage. Debris too large to pass through the culvert accu-

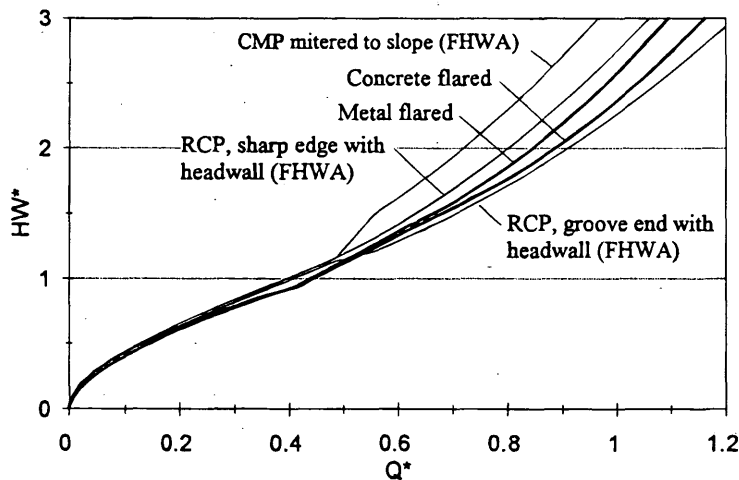


FIGURE 5 Comparison of inlet-control rating curves for four types of end sections.

mulates at the water surface around the inlet. As the headwater rises, the top of the inlet traps some of this debris; the rest floats on the water surface above the inlet. At higher discharges, the debris around the inlet is compacted and drawn further into the culvert. As the storm flow recedes and the headwater falls, the floating debris settles in front of the inlet. After a flood, a culvert inlet may be entirely covered with debris.

Additional experiments were conducted to quantify the hydraulic effects of the floating debris. The metal end sections were used for these tests because they have sharper inlet edges and consequently have a greater tendency to snag and hold debris. The original experiments for inlet-control flow and for full flow were repeated with debris. The same amount of debris was used in each experiment. The end section was allowed to plug naturally.

The inlet-control tests with debris yielded some unexpected results. The debris had only a slight adverse effect on the hydraulic capacities of the metal flared end sections in repeated tests. Figure 6 shows the results from a typical test of a metal end section with debris. The concrete flared end section actually conveyed more flow with debris than without debris. Figure 7 shows the results from a typical test of a concrete end section with debris. In this test, the culvert began to flow full at $HW/D \approx 1.5$. Without debris, the culvert did not flow full at any headwater depth. Apparently the accumulated debris suppresses the downward component of the inflow and the vortex at the inlet. These changes in the flow pattern around the inlet are conducive to full flow.

An accumulation of debris around the inlet obviously increases the entrance loss. The entrance-loss coefficients for full flow are considerably higher with debris than without debris. The model tests with debris yielded average entrance-loss coefficients of 0.65 for the metal flared end sections and 1.05 for the concrete flared end sections.

In summary, the hydraulic impact of floating debris depends on whether the culvert would operate under inlet control or outlet control without debris. If the culvert would operate under inlet control

without debris, the debris can cause the culvert to flow full and thereby increase its hydraulic performance. If the culvert would operate under outlet control without debris, then debris would only increase the entrance loss and thereby reduce the culvert's capacity.

IMPROVED HYDRAULIC PERFORMANCE WITH FLOW BARS

The results of the tests with debris provided insight into the hydraulic behavior of the flared end sections. Much of the inflow has a strong downward velocity component. The downward momentum of the inflow causes severe contraction of the flow directly downstream of the inlet, which limits the amount of flow that can enter the pipe. Therefore, any measure that reduces the downward momentum of the inflow should increase the discharge capacity of the culvert under inlet control.

It was found that the hydraulic performance of flared inlets could be improved markedly by the addition of "flow bars" across the top third of the inlet opening, as shown in Figure 8. These bars reduce the downward momentum of the inflow and thus lessen the contraction of the flow directly downstream of the inlet. The model of the 152-cm (60-in.) metal end section was tested with many different arrangements of flow bars. Figure 8 shows the arrangement that worked best. Figure 9 shows the dimensionless inlet-control rating curves for metal flared end sections with and without flow bars. The most important difference is that the metal flared end section with the flow bars forced the short smooth pipe to flow full at $HW/D > 1.7$. [Certain other types of end sections will also force a short smooth pipe to flow full. Examples include the hood inlet (7) and metal safety-sloped end sections (8).] Flared end sections without flow bars did not cause the pipe to flow full at any headwater. The flow bars also make the inlet slightly more efficient when submerged and operating under inlet control. The dimension-

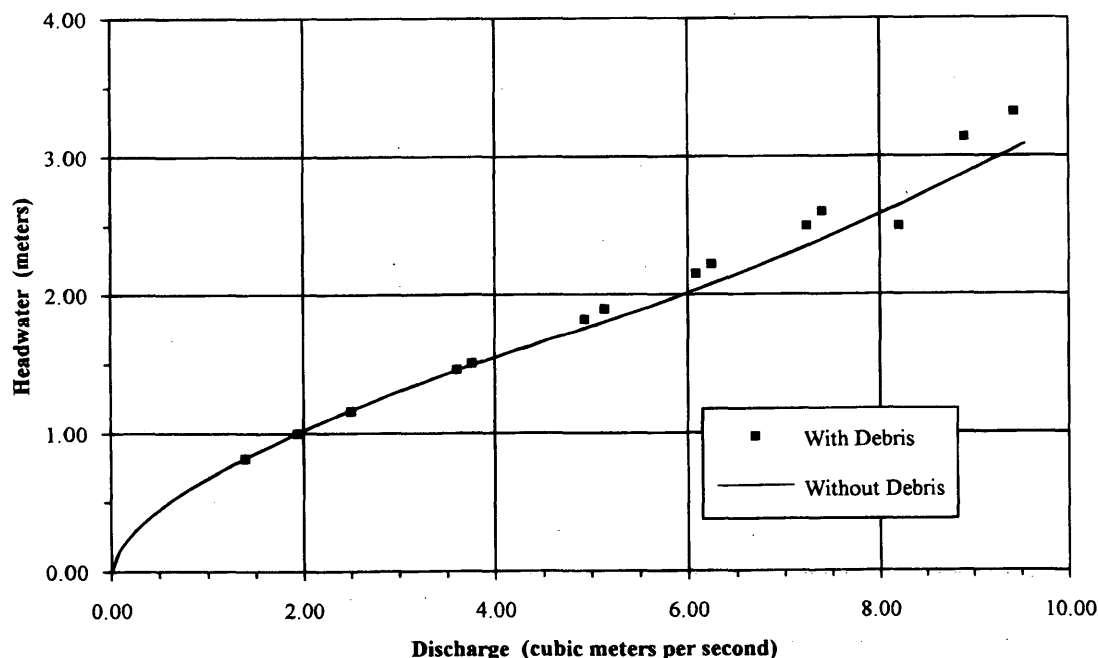


FIGURE 6 Hydraulic performance of 152-cm (60-in.) metal flared end section with floating debris.

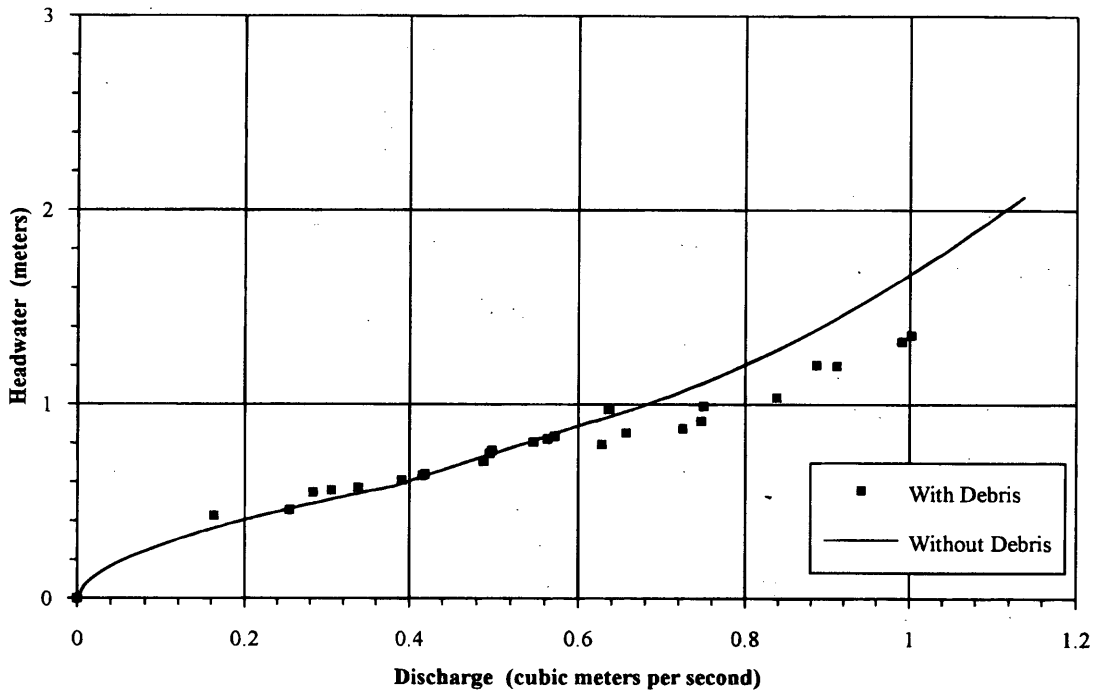
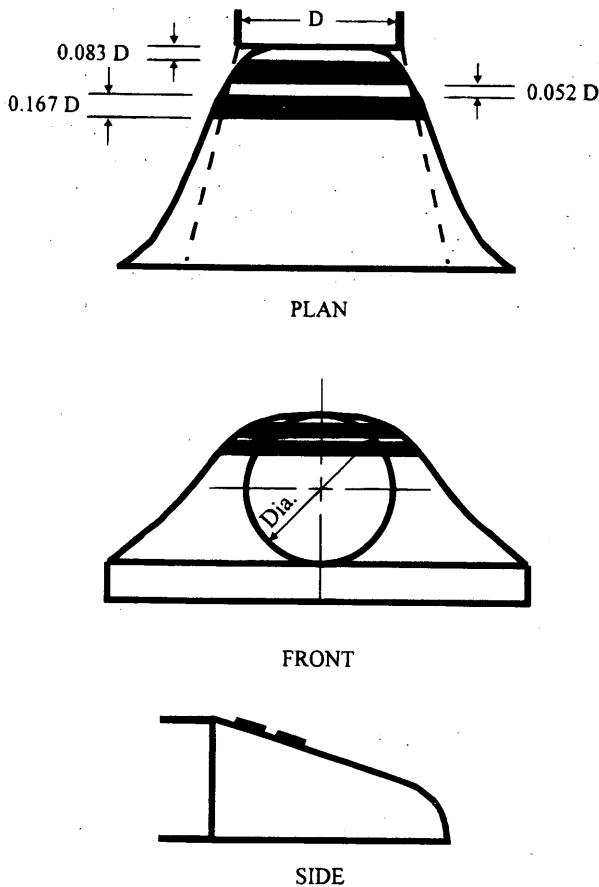


FIGURE 7 Hydraulic performance of 152-cm (60-in.) concrete flared end section with floating debris.



less rating curve for the metal flared inlet with flow bars is fitted by the equation

$$HW^* = \begin{cases} 1.60 (Q^*)^{0.60} & 0 \leq Q^* \leq 0.41 \\ 0.578 + 0.26 (Q^*) + 1.50 (Q^*)^2 & 0.41 \leq Q^* \leq 0.78 \end{cases} \quad (8)$$

The outlet-control tests yielded an entrance-loss coefficient of 0.42 for the 152-cm (60-in.) metal flared end section with flow bars. No tests were run on concrete flared inlets with flow bars. However, it was expected that flow bars would have roughly the same effects on concrete end sections as on metal end sections. The tests indicate that flow bars could improve the hydraulic performance of any culvert with a flared end section that would otherwise operate under inlet control (e.g., most large concrete culverts). Flow bars would not be beneficial on a culvert that would flow full anyway.

As an illustration of the potential benefit of flow bars in a favorable situation, Figure 10 compares the rating curves for two identical culverts with metal flared end sections, one with flow bars and the other without flow bars. The culvert is a 152-cm (60-in.) concrete pipe 15 m (50 ft) long with a bottom slope of 0.05 m/m and a Manning *n* of 0.012. The tailwater level is below the level of critical flow in the pipe at all discharges.

The culvert with the flow bars would operate under inlet control only up to $HW^* \approx 1.7$, or $HW = 2.6$ m (8.5 ft). At greater headwater depths, it would flow full. The culvert without the flow bars would operate under inlet control at all discharges. These culverts operate more efficiently under full flow than under inlet control. By forcing full flow at headwater depths above 2.6 m (8.5 ft), the flow bars greatly increase the culvert's discharge capacity. For example, at a headwater depth of 3.0 m (10 ft), the flow bars increase the discharge capacity by 35 percent, from 7.1 m³/sec (250 ft³/sec) to 9.6 m³/sec (340 ft³/sec).

FIGURE 8 Optimum arrangement of flow bars for metal flared end section.

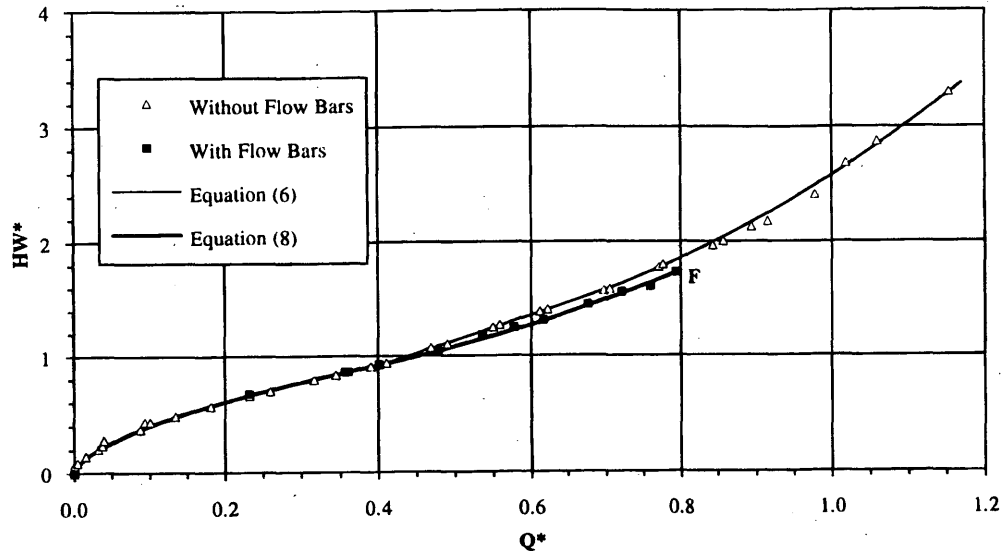


FIGURE 9 Comparison of inlet-control rating curves for 152-cm (60-in.) metal flared end section with and without flow bars.

SUMMARY AND CONCLUSIONS

Under inlet control, standard flared end sections perform much better than mitered pipes, slightly better than headwalls with sharp inlet edges, and slightly worse than headwalls with grooved or rounded inlet edges. The concrete flared end sections are slightly more efficient than the metal end sections. Inlet-control rating curves for standard flared end sections of all sizes can be developed from Equations 6 and 7. A standard flared end section will not force a pipe culvert to flow full, although it may flow full for another reason (high tailwater or internal friction). The entrance-loss coefficients for flared end sections range from 0.24 to 0.30. The larger end sections have slightly lower entrance-loss coefficients than the smaller end sections.

Floating debris has little effect on the hydraulic performance of the flared end sections under inlet control. However, an accumula-

tion of debris at the inlet serves to suppress vortices and reduce the downward momentum of the inflow. These effects can cause a shift from inlet control to full flow, a more efficient operating condition. If a culvert flows full anyway because of high tailwater or internal friction, floating debris only increase the entrance loss.

The hydraulic performance of a flared inlet can be improved by adding flow bars across the top third of the inlet opening. The flow bars have the same hydraulic effects as an accumulation of debris at the inlet. Tests indicate that a metal flared inlet with the flow bar arrangement in Figure 10 will force even a short smooth pipe to flow full whenever the headwater depth exceeds 170 percent of the pipe diameter. The flow bars also make the flared end section slightly more efficient under inlet control. The only disadvantage of the flow bars is a slight increase in the entrance loss for full flow. Most concrete pipe culverts with flared inlets would benefit from the addition of flow bars.

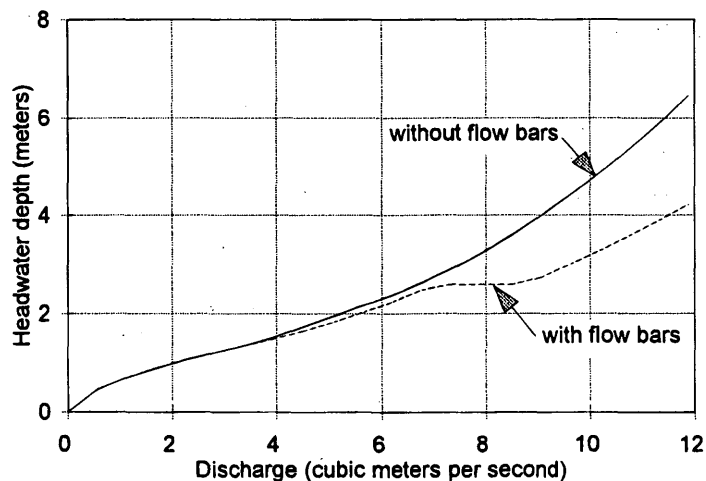


FIGURE 10 Rating curves for pipe culvert with flared end sections with and without flow bars.

ACKNOWLEDGMENT

This project was supported by KDOT through the K-TRAN Cooperative Transportation Research Program. The project monitor was James Richardson, Senior Road Squad Leader, KDOT.

REFERENCES

1. Normann, J. M., R. J. Houghtalen, and W. J. Johnston. *Hydraulic Design of Highway Culverts*. Hydraulic Design Series 5, Report FHWA-IP-85-15, FHWA, U.S. Department of Transportation, 1985.
2. Blaisdell, F. W. Hydraulic Efficiency in Culvert Design (closure). *Journal of the Highway Division*, American Society of Civil Engineers, Vol. 93, No. HW2, Nov. 1967, pp. 192-194.
3. Blaisdell, F. W. Flow in Culverts and Related Design Philosophies (closure). *Journal of the Hydraulics Division*, American Society of Civil Engineers, Vol. 94, No. HY2, March 1968, pp. 531-540.
4. Blaisdell, F. W., and C. A. Donnelly. Tapered Inlets for Pipe Culverts (discussion). *Journal of the Hydraulics Division*, American Society of Civil Engineers, Vol. 90, No. HY6, Nov. 1964, pp. 315-324.
5. Ree, W. O., and C. E. Rice. Tapered Inlets for Pipe Culverts (discussion). *Journal of the Hydraulics Division*, American Society of Civil Engineers, Vol. 90, No. HY6, Nov. 1964, pp. 329-330.
6. Rice, C. E. Effect of Pipe Boundary on Hood Inlet Performance. *Journal of the Hydraulics Division*, American Society of Civil Engineers, Vol. 93, No. HY4, July 1967, pp. 149-167.
7. Blaisdell, F. W. Hood Inlet for Closed Conduit Spillways. *Journal of the Hydraulics Division*, American Society of Civil Engineers, Vol. 86, No. HY5, May 1960, pp. 7-31.
8. McEnroe, B. M. Hydraulics of Safety End Sections for Highway Culverts. *Transportation Research Record 1471*, TRB, National Research Council, Washington, D.C., 1994.